Published in final edited form as:
Nano Lett. 2020 November 11; 20(11): 8163–8169. doi:10.1021/acs.nanolett.0c03260.

Rapid Structural, Kinetic and Immunochemical Analysis of Alpha-Synuclein Oligomers in Solution

William E. Arter[#1,2], **Catherine K. Xu**[#1], **Marta Castellana-Cruz**[1], **Therese W. Herling**[1], **Georg Krainer**[1], **Kadi L. Saar**[1], **Janet R. Kumita**[1], **Christopher M. Dobson**[1,i], **Tuomas P. J. Knowles**[1,2,*]

[1]Department of Chemistry, University of Cambridge, Lensfield Road, Cambridge CB2 1EW UK

[2]Cavendish Laboratory, University of Cambridge, JJ Thomson Avenue, Cambridge CB3 0HE, UK

[#] These authors contributed equally to this work.

Abstract

Oligomers comprised of misfolded proteins are implicated as neurotoxins in the pathogenesis of protein misfolding conditions such as Parkinson's and Alzheimer's diseases. Structural, biophysical, and biochemical characterisation of these nanoscale protein assemblies is key to understanding their pathology and the design of therapeutic interventions, yet is challenging due to their heterogeneous, transient nature and low relative abundance in complex mixtures. Here, we demonstrate separation of heterogeneous populations of oligomeric α-synuclein, a protein central to the pathology of Parkinson's disease, in solution using microfluidic free-flow electrophoresis. We characterise nanoscale structural heterogeneity of transient oligomers on a timescale of seconds, at least two orders of magnitude faster than conventional techniques. Furthermore, we utilise our platform to analyse oligomer ζ-potential and probe the immunochemistry of wild-type α-synuclein oligomers. Our findings contribute to an improved characterisation of alpha-synuclein oligomers and demonstrate the application of microchip electrophoresis for the free-solution analysis of biological nanoparticle analytes.

Keywords

Alpha-synuclein; oligomer; microfluidics; free-flow electrophoresis; aptamer

Introduction

Protein misfolding is a molecular hallmark of a number of increasingly prevalent human diseases.[1] Amyloid fibrils formed from misfolded proteins are the major components of the Lewy bodies and senile plaques found in the brains of patients with neurodegenerative conditions such as Parkinson's and Alzheimer's diseases, respectively.[2] However, fibrillar

[*]Corresponding author. tpjk2@cam.ac.uk.
[i]Deceased September 2019

Author Contributions

W.E.A, C.K.X, J.R.K, C.M.D, T.P.J.K designed research, W.E.A, C.K.X performed research, M.C.C, T.W.H, K.L.S contributed reagents/analytic tools, W.E.A, C.K.X analyzed data and W.E.A, C.K.X, G.K, J.R.K, T.P.J.K wrote the paper.

species possess low inherent toxicity themselves, and it is instead pre-fibrillar, oligomeric aggregates that are implicated as the principal cytotoxic agents in these disorders.[3–5] The characterisation and quantitation of these protein nanoparticles in the context of their toxicity and aggregation propensity is therefore an area of intense interest.[6,7] However, deciphering the structural attributes of oligomeric species, which exist as an intrinsically heterogenous population of structures during protein aggregation, is hard to achieve using established methods that report the properties of analyte mixtures in an ensemble-averaged manner. Although measurements of oligomer populations, taken throughout protein aggregation processes, have enabled coarse-grained relationships between structure and toxicity to be defined,[8,9] they do not permit detailed characterisation of oligomer properties including ζ-potential, which may also play a crucial role in determining oligomer aggregation propensity.[10] Furthermore, oligomers exist in a complex, dynamic milieu of protein–protein interactions, but current methodologies are often incapable of probing such systems on a timescale relevant to temporal changes in oligomer populations.[11] Crucially, current methods for the separation of heterogeneous protein mixtures such as size exclusion chromatography (SEC), analytical ultracentrifugation (AUC) and native gel electrophoresis operate on timescales of minutes to hours, limiting temporal resolution. This feature is particularly important when analysing protein oligomers, since oligomer populations undergo continuous change throughout the aggregation process. In addition, existing techniques for oligomer analysis often perturb the system in question by dilution[12] or use of non-solution state approaches,[13,14] which may alter the oligomer properties that are observed due to dilution-driven dissociation or interaction with the surface.

To address these challenges, we have developed an approach based upon multi-spectral microchip free-flow electrophoresis (μFFE) that achieves rapid solution-phase fractionation and in-situ analysis of heterogeneous mixtures of protein oligomers and monomers. Our approach enables second timescale separation and solution-phase analysis of oligomer mixtures, at least two orders of magnitude faster than conventional techniques. We focus on the aggregation and oligomerisation of alpha-synuclein (αS), a protein that is strongly implicated in the pathogenesis of Parkinson's disease.[15] Using this approach, complex oligomeric mixtures are fractionated on-chip to afford rapid oligomer quantification and characterisation of ensemble heterogeneity, whilst allowing simultaneous measurement of oligomer ζ-potential, a hitherto inaccessible parameter. In addition, the short experimental timescale (analysis time ~5 s), solution-phase conditions and minimal sample dilution enable an accurate, native-state snapshot of dynamic oligomer populations with high temporal resolution.

First, we demonstrate the principle of our method through analysis of stable, fluorophore-labelled kinetically trapped αS oligomers that have been characterised in detail previously,[11] before applying the technique to the analysis of transient oligomers that arise during protein aggregation. Moreover, by use of an oligomer-selective aptamer probe, we further demonstrate the broad applicability of our method by investigation of wild-type, unlabelled αS oligomers.

Results and Discussion

Our microchip electrophoretic approach is based on a μFFE[16,17] platform[18] that allows rapid fractionation of samples containing a complex mixture of oligomeric and monomeric proteins (Figure 1(a)). The sample, flanked by an auxiliary buffer, is passed under laminar flow through the microfluidic chip whilst an electric field is applied perpendicular to the flow direction, resulting in fractionation of the heterogeneous mixture according to the different electrophoretic mobilities of the sample components (Figure 1(b)). Notably, our device incorporates an in-line microfluidic sample-desalting[19,20] module for rapid (~2 s) sample preparation on chip (Figure S1, Supporting Information). This enables the use of high-salt, physiologically-relevant buffers such as phosphate buffered saline (PBS), which are otherwise inaccessible in μFFE, as excessive ionic conduction through the buffer prevents the application of electric field. To allow facile in-situ differentiation between monomeric and oligomeric αS fractions (Figure 1(b)), αS monomer labelled with a fluorophore (Alexa546) orthogonal to that of the oligomeric protein mixture (Alexa488) is introduced as an in-situ reference. For this approach to be effective, it is necessary for both αS labelling variants to possess the same electrophoretic mobility; hence, the dyes were chosen due to their same inherent charge,[21] and quantification of the mobilities of the two labelling variants confirmed that they were identical, with $\mu = -1.43 \pm 0.11 \times 10^{-8}\ m^2\ V^{-1}\ s^{-1}$ (Figure S2). Moreover, comparative analysis of fluorophore-labelled and wild-type αS oligomers by circular dichroism, Fourier transform infra-red spectroscopy and transmission electron microscopy indicated almost identical structural characteristics between the oligomer variants (Figure S4, Supporting Information).

We initially demonstrate separation of αS monomers from kinetically-trapped, stable αS oligomers prepared both in high and low-salt conditions (Figure 1(c)). Mixtures of kinetically stable, Alexa488-labelled oligomers together with both Alexa488 and 546-labelled monomer in PBS or 10 mM sodium phosphate buffer were analysed. Two distinct fractions were observed for the oligomeric mixture (Alexa488), but only a single fraction was present for the monomer-only sample (Alexa546). By comparison to the Alexa546 fluorescence profile, the lower and higher mobility fractions could be clearly identified as monomeric and oligomeric protein, respectively (Figure 1↓(d, e)). As expected, a broad peak width is observed for monomer, resulting from faster diffusion due to its smaller hydrodynamic radius in comparison to oligomeric species. Indeed, further analysis revealed significant oligomer heterogeneity, with a similar electrophoretic profile for both conditions comprising a major oligomer population at $\mu = -2.49 \pm 0.16 \times 10^{-8}\ m^2\ V^{-1}\ s^{-1}$ combined with a significant high-mobility shoulder composed of smaller sub-populations.

We attribute the electrophoretic separation of oligomer and monomer to the faster scaling of effective oligomer charge relative to oligomer size, for an oligomer of n_m monomer units. Oligomer electrophoretic mobility (μ_o) is proportional to oligomer charge (q_o) and inversely proportional to oligomer hydrodynamic radius (r_o) according to $\mu_o \propto \frac{q_o}{r_o} \propto \frac{n_m^v}{r_o}$, where v is a scaling exponent that links q_o with n_m. αS oligomers have been reported to possess an approximately spherical morphology,[11,22,23] and we approximate that

$n_m \approx \frac{v_o}{v_m} = \frac{r_o^3}{r_m^3}$ where V_o, V_m, r_o and r_m represent the oligomer and monomer volumes and oligomer and monomer hydrodynamic radii, respectively. Together, these expressions yield the oligomer electrophoretic mobility as a function of n_m according to Equation 1, where $\nu^* = \nu - \frac{1}{3}$. According to this relationship, oligomers are expected to have higher mobilities than monomeric protein, and oligomer mobility is predicted to increase with oligomer size. Additional data, definition of apparent mobility and further discussion of desalting-μFFE are provided in the Supporting Information.

$$\mu_o \propto \frac{n_m^{\nu}}{r_m n_m^{1/3}} = \frac{n_m^{\nu^*}}{r_m} \quad (1)$$

To verify this size–mobility relationship, we compared μFFE to AUC, which is an established technique for the analysis of size distributions within complex samples. A similar oligomer profile was consistently observed in both the AUC and μFFE analyses, indicating a scaling of oligomer electrophoretic mobility with oligomer size (Figure 1(f), additional data and rationalisation are provided in the SI). This observation shows that the electropherograms generated through μFFE correspond directly to size distributions of component species, as predicted by Equation 1, thus validating the μFFE approach as a tool for the analysis of oligomer structural heterogeneity. From the AUC analysis, values of r_o were found to be in the range 5.8-11 nm, in agreement with those determined previously.[11]

Having shown that our μFFE approach enables the fractionation of oligomeric protein mixtures, we analysed the resultant oligomer electropherograms to access oligomer ζ-potentials, a fundamental parameter of nanoscale aggregates. The ζ-potential describes interactions between particles, where it modulates the propensity of the system to aggregate further, and between aggregates and other biological components such as cell membranes. Previously, this parameter has been challenging to study for oligomeric protein aggregates, due to the high degree of structural heterogeneity intrinsic in oligomer samples that confounds conventional techniques, such as dynamic light scattering, for ζ-potential analysis.[24] Since our method allows direct observation of oligomer heterogeneity during free-solution electrophoresis, ζ-potentials can be accurately assigned to the major oligomer population rather than to the population average. Following normalisation, the monomer-only Alexa546 profile was subtracted from the Alexa488 signal to yield an electropherogram corresponding to oligomeric species only, and values for oligomer ζ-potential were extracted from the reported electrophoretic mobilities (Figure 1(e), see SI).[25] The most common oligomer ζ-potential of $\zeta = -42.6 \pm 4.1$ mV is characteristic of particulate systems with high colloidal stability.[26,27] This finding is significant as it supports the view of protein oligomers as species that do not undergo aggregation themselves.[28] The stability we observe suggests that these oligomers will not be removed from solution by flocculation or aggregation, consistent with them existing as a kinetically-trapped,[11] long-lived colloidal suspension, with implications for the longevity of oligomer cellular toxicity.[5,11,29]

Europe PMC Funders Author Manuscripts

Notably, despite the relationship between surface charge and colloidal stability being of clear relevance to oligomer behaviour, few experimental studies have attempted to quantify ζ-potential within heterogeneous oligomer populations, likely due to the challenges such an experiment would present for established techniques.[30] The μFFE method offers a facile method for quantifying this parameter in protein aggregation systems, introducing an important parameter for understanding the physical-chemical nature of aggregate species.

Following our analysis of kinetically-trapped, stable oligomers, we applied our μFFE platform to the study of transient αS oligomers formed during protein aggregation. Aliquots were periodically withdrawn from the shaking-initiated aggregation reaction of Alexa488-labelled αS monomer, fibrillar components were removed by centrifugation before the samples were analysed by μFFE. High-mobility fractions in the aggregation mixture corresponding to oligomeric αS could be identified and quantified (Figure 2(a, b, c)), following comparison of the electrophoresis profiles for the aggregation mixture and the Alexa546-labelled monomer reference, which yielded electropherograms corresponding to oligomeric αS alone (Figure 2(d)).

No oligomers were observed prior to aggregation initiation, before their concentration increased through the lag phase of the reaction, reaching a peak concentration of 1.75 μM (monomer equivalent) out of a total αS concentration of 100 μM with concomitant initiation of protein fibrillisation after 36h. This behaviour is in good agreement with studies employing single-molecule Förster resonance energy transfer (smFRET) experiments.[31] Furthermore, two distinct oligomeric subpopulations are observable in the aggregation time course, which corresponds well with smFRET experiments where two major subpopulations of αS oligomers have been observed.[8,9] Oligomers with low FRET efficiency formed first in the aggregation reaction, before converting to species with high FRET efficiency, suggesting a more densely packed structure. Our finding that low mobility species evolve to form high mobility species is thus consistent with an increase in packing efficiency, corresponding to a decrease in hydrodynamic radius.

However, smFRET techniques require up to 10^5-fold sample dilution, which may result in under-sampling of transient, weakly-bound oligomer species that are prone to dissociation.[12,32] In contrast, sample dilution is not required for μFFE, enabling accurate oligomer quantitation as evidenced by close agreement with values obtained by other techniques such as size exclusion chromatography.[33] Notably, the μFFE experiment (≈ 5 s analysis time) is three orders of magnitude faster than methods such as AUC. This crucial feature allowed access to transient species that would be otherwise challenging to observe by AUC or other bulk separation methods, with minimal sample consumption of only a few μL.

In addition to these approaches, previous studies have employed micro-capillary electrophoresis (MCE) techniques[34,35] to analyse protein aggregation products; these works were primarily focused on the observation of fibrillar species rather than oligomers[36] or were non-quantitative.[37,38] While MCE techniques generally provide advantages in terms of resolution relative to μFFE,[39,40] they pose challenges in the quantitation of rare species, due to the injection of a finite volume of sample. In contrast, the steady-state, continuous fractionation process intrinsic to μFFE prevents sample bleaching during data acquisition

and enhances sensitivity through the use of arbitrary exposure time in conventional epifluorescence microscopy. These advantages over MCE techniques are key to our application of μFFE to detecting and characterising lowly populated oligomeric species in aggregation reactions.

Further to the fluorophore-tagged protein systems discussed so far, μFFE can be employed for the analysis of wild-type oligomeric species when used in conjunction with an appropriate oligomer-binding probe. We demonstrate this capability by utilising a fluorophore-tagged aptamer selective for αS oligomers.[41] As shown previously,[42] protein–aptamer binding retards the electrophoretic mobility of the aptamer, enabling separation of the bound and unbound fractions (Figure 3(a)). Aliquots taken from stirring-induced aggregation of wild-type αS were incubated with the aptamer and analysed by μFFE (Figure 3(b)). After 4.25 h aggregation time, an additional fraction at lower mobility than the unbound aptamer was observed. By peak integration and assuming 1:1 binding stoichiometry, an upper bound of 80 nM oligomer concentration could be estimated (Figure 3(c)). By comparison to the maximal monomer-equivalent concentration of labelled oligomer observed previously (Figure 2(c)), it could be approximated that around twenty monomer units are present in each oligomer, in good agreement with previously ascertained values.[11] The oligomeric nature of the peak was confirmed by μFFE of the aptamer in the presence of αS monomer alone and sonicated αS fibrils (Supporting Information). These data show that label-free, wild-type oligomers can be observed and quantified by μFFE, and demonstrates the versatility of our method towards applications involving immunochemistry-based oligomer detection and manipulation.

Conclusion

Oligomeric proteins are heavily implicated as toxic agents in protein-misfolding diseases. Understanding oligomer structure, heterogeneity, and physical properties in solution conditions is of vital importance to elucidate relationships between oligomer structure and toxicity, and to enable the design of effective therapeutics.

The μFFE platform presented here is a multifaceted tool for the observation and analysis of these pre-fibrillar intermediates in free solution and physiological conditions. Using this approach, we demonstrate characterisation of oligomer structural heterogeneity within populations of both kinetically-stabilised and transient, on-pathway oligomers isolated from aggregation reaction mixtures. Crucially, on-chip sample preparation and the rapid experimental timescale enabled by the μFFE platform results in minimal sample perturbation and very high temporal resolution. We quantify oligomer zeta-potential, with our results indicating a high degree of oligomer colloidal stability, supporting the view that oligomers are relatively long-lived species with a low propensity to directly aggregate themselves. Significantly, we observe an interaction between wild-type oligomers and an immuno-probe in free solution. These properties are fundamental to both the physical and biological understanding of oligomer behaviour, but are challenging to study using conventional methods due to the intrinsic heterogeneity of oligomer samples.

Europe PMC Funders Author Manuscripts

Oligomer μFFE has many potential applications, such as in the analysis of protein aggregation kinetics, the links between oligomer structure and toxicity, and for screening protein–protein and protein–small molecule interactions in the development of therapeutic interventions for misfolding disease. More broadly, our findings demonstrate the suitability of free-flow electrophoretic methods for the quantitative, free-solution analysis of nanoparticle analytes in general, according to their size and surface properties.

Supplementary Material

Refer to Web version on PubMed Central for supplementary material.

Acknowledgment

The research leading to these results has received funding from the European Research Council under the European Union's Seventh Framework Programme (FP7/2007-2013) through the ERC grant PhysProt (agreement 337969) and from the Newman Foundation. W. E. A. acknowledges support from the EPSRC Cambridge NanoDTC, EP/L015978/1. C.K.X acknowledges support from a Herchel Smith Research Studentship. T.W.H. acknowledges support from the Oppenheimer Fund and the BBSRC. G.K. has received funding from the European Research Council under the European Union's Horizon 2020 Framework Programme through the Marie Sklodowska-Curie grant MicroSPARK (agreement n° 841466). K.L.S. acknowledges support from the EPSRC. All authors are supported by the Centre for Misfolding Diseases.

References

1. Chiti F, Dobson CM. Protein Misfolding, Amyloid Formation, and Human Disease: A Summary of Progress Over the Last Decade. Annu Rev Biochem. 2017; 86:27–68. [PubMed: 28498720]
2. Masters CL, et al. Amyloid plaque core protein in Alzheimer disease and Down syndrome. Proc Natl Acad Sci. 1985; 82:4245–4249. [PubMed: 3159021]
3. Haass C, Selkoe DJ. Soluble protein oligomers in neurodegeneration: lessons from the Alzheimer's amyloid β-peptide. Nat Rev Mol Cell Biol. 2007; 8:101–112. [PubMed: 17245412]
4. Benilova I, Karran E, De Strooper B. The toxic Aβ oligomer and Alzheimer's disease: an emperor in need of clothes. Nat Neurosci. 2012; 15:349–357. [PubMed: 22286176]
5. Ingelsson M. Alpha-Synuclein Oligomers: Neurotoxic Molecules in Parkinson's Disease and Other Lewy Body Disorders. Front Neurosci. 2016; 10:408. [PubMed: 27656123]
6. Bengoa-Vergniory N, Roberts RF, Wade-Martins R, Alegre-Abarrategui J. Alpha-synuclein oligomers: a new hope. Ada Neuropathol. 2017; 134:819–838.
7. Ono K. The Oligomer Hypothesis in α-Synucleinopathy. Neurochem Res. 2017; 42:3362–3371. [PubMed: 28828740]
8. Cremades N, et al. Direct observation of the interconversion of normal and toxic forms of α-synuclein. Cell. 2012; 149:1048–59. [PubMed: 22632969]
9. Iljina M, et al. Kinetic model of the aggregation of alpha-synuclein provides insights into prion-like spreading. Proc Natl Acad Sci U S A. 2016; 113:E1206–15. [PubMed: 26884195]
10. Li X, et al. Early stages of aggregation of engineered α-synuclein monomers and oligomers in solution. Sci Rep. 2019; 9:1734. [PubMed: 30741954]
11. Chen SW, et al. Structural characterization of toxic oligomers that are kinetically trapped during α-synuclein fibril formation. Proc Natl Acad Sci U S A. 2015; 112:E1994–2003. [PubMed: 25855634]
12. Whiten DR, et al. Single-Molecule Characterization of the Interactions between Extracellular Chaperones and Toxic α-Synuclein Oligomers. Cell Rep. 2018; 23:3492–3500. [PubMed: 29924993]
13. Simone Ruggeri F, Habchi J, Cerreta A, Dietler G. AFM-Based Single Molecule Techniques: Unraveling the Amyloid Pathogenic Species. Curr Pharm Des. 2016; 22:3950–3970. [PubMed: 27189600]

14. Pieri L, Madiona K, Melki R. Structural and functional properties of prefibrillar α-synuclein oligomers. Sci Rep. 2016; 6:24526. [PubMed: 27075649]
15. Stefanis L. alpha-synuclein and Lewy pathology in Parkinson's disease. Cold Spring Harb Perspect Med. 2012; 4
16. Turgeon RT, Bowser MT. Micro Free-Flow Electrophoresis: Theory and Applications. Anal Bioanal Chem. 2009; 394:187–198. [PubMed: 19290514]
17. Herling TW, Arosio P, Müller T, Linse S, Knowles TPJ. A Microfluidic Platform for Quantitative Measurements of Effective Protein Charges and Single Ion Binding in Solution. Phys Chem Chem Phys. 2015; 17:12161–12167. [PubMed: 25880209]
18. Saar KL, et al. On Chip Label Free Protein Analysis with Downstream Electrodes for Direct Removal of Electrolysis Products. Lab Chip. 2018; 18:162–170.
19. Tibavinsky IA, Kottke PA, Fedorov AG. Microfabricated ultrarapid desalting device for nanoelectrospray ionization mass spectrometry. Anal Chem. 2015; 87:351–356. [PubMed: 25490085]
20. Wilson DJ, Konermann L. Ultrarapid desalting of protein solutions for electrospray mass spectrometry in a microchannel laminar flow device. Anal Chem. 2005; 77:6887–6894. [PubMed: 16255586]
21. Zanetti-Domingues LC, Tynan CJ, Rolfe DJ, Clarke DT, Martin-Fernandez M. Hydrophobic Fluorescent Probes Introduce Artifacts into Single Molecule Tracking Experiments Due to Non-Specific Binding. PLoS One. 2013; 8
22. van Diggelen F, et al. Two conformationally distinct α-synuclein oligomers share common epitopes and the ability to impair long-term potentiation. PLoS One. 2019; 14
23. Andreasen M, Lorenzen N, Otzen D. Interactions between misfolded protein oligomers and membranes: A central topic in neurodegenerative diseases? Biochim Biophys Acta - Biomembr. 2015; 1848:1897–1907.
24. Arosio P, et al. Microfluidic Diffusion Analysis of the Sizes and Interactions of Proteins under Native Solution Conditions. ACS Nano. 2016; 10:333–341. [PubMed: 26678709]
25. Doane TL, Chuang C-H, Hill RJ, Burda C. Nanoparticle ζ-Potentials. Acc Chem Res. 2011; 45:317–326. [PubMed: 22074988]
26. Jiang J, Oberdörster G, Biswas P. Characterization of size, surface charge, and agglomeration state of nanoparticle dispersions for toxicological studies. J Nanoparticle Res. 2009; 11:77–89.
27. Joseph, E, Singhvi, G, Grumezescu, AM. Nanomaterials for Drug Delivery and Therapy. First. Elsevier Science Publishing Inc; 2019.
28. Lashuel HA, Overk CR, Oueslati A, Masliah E. The many faces of α-synuclein: From structure and toxicity to therapeutic target. Nature Reviews Neuroscience. 2013; 14:38–48. [PubMed: 23254192]
29. Danzer KM, et al. Different species of alpha-synuclein oligomers induce calcium influx and seeding. J Neurosci. 2007; 27:9220–32. [PubMed: 17715357]
30. Stetefeld J, McKenna SA, Patel TR. Dynamic light scattering: a practical guide and applications in biomedical sciences. Biophys Rev. 2016; 8:409–427. [PubMed: 28510011]
31. Iljina M, et al. Nanobodies raised against monomeric a-synuclein inhibit fibril formation and destabilize toxic oligomeric species. BMC Biol. 2017; 15:57. [PubMed: 28673288]
32. Kjaergaard M, et al. Oligomer Diversity during the Aggregation of the Repeat Region of Tau. ACS Chem Neurosci. 2018; 9:3060–3071. [PubMed: 29953200]
33. Cremades N, et al. Direct Observation of the Interconversion of Normal and Toxic Forms of α-Synuclein. Cell. 2012; 149:1048–1059. [PubMed: 22632969]
34. Harstad RK, Johnson AC, Weisenberger MM, Bowser MT. Capillary Electrophoresis. Anal Chem. 2015; 88:299–399. [PubMed: 26640960]
35. Voeten RLC, Ventouri IK, Haselberg R, Somsen GW. Capillary Electrophoresis: Trends and Recent Advances. Anal Chem. 2018; 90:1464–1481. [PubMed: 29298038]
36. Picou RA, et al. Separation and detection of individual Aβ aggregates by capillary electrophoresis with laser-induced fluorescence detection. Anal Biochem. 2012; 425:104–112. [PubMed: 22446499]

37. Sabella S, et al. Capillary electrophoresis studies on the aggregation process ofβ-amyloid 1-42 and 1-40 peptides. Electrophoresis. 2004; 25:3186–3194. [PubMed: 15472964]
38. Napp A, et al. Separation and determination of alpha-synuclein monomeric and oligomeric species using two electrophoretic approaches. Electrophoresis. 2018; 39:3022–3031. [PubMed: 30157293]
39. Fonslow BR, Bowser MT. Optimizing band width and resolution in micro-free flow electrophoresis. Anal Chem. 2006; 78:8236–8244. [PubMed: 17165812]
40. Zhang Z, Zhang F, Liu Y. Recent advances in enhancing the sensitivity and resolution of capillary electrophoresis. J Chromatogr Sci. 2013; 51:666–683. [PubMed: 23515192]
41. Tsukakoshi K, Abe K, Sode K, Ikebukuro K. Selection of DNA Aptamers That Recognize a-Synuclein Oligomers Using a Competitive Screening Method. Anal Chem. 2012; 84:5542–5547. [PubMed: 22697251]
42. Arter WE, et al. Combining Affinity Selection and Specific Ion Mobility for Microchip Protein Sensing. Anal Chem. 2018; 90:10302–10310. [PubMed: 30070105]

Europe PMC Funders Author Manuscripts

Europe PMC Funders Author Manuscripts

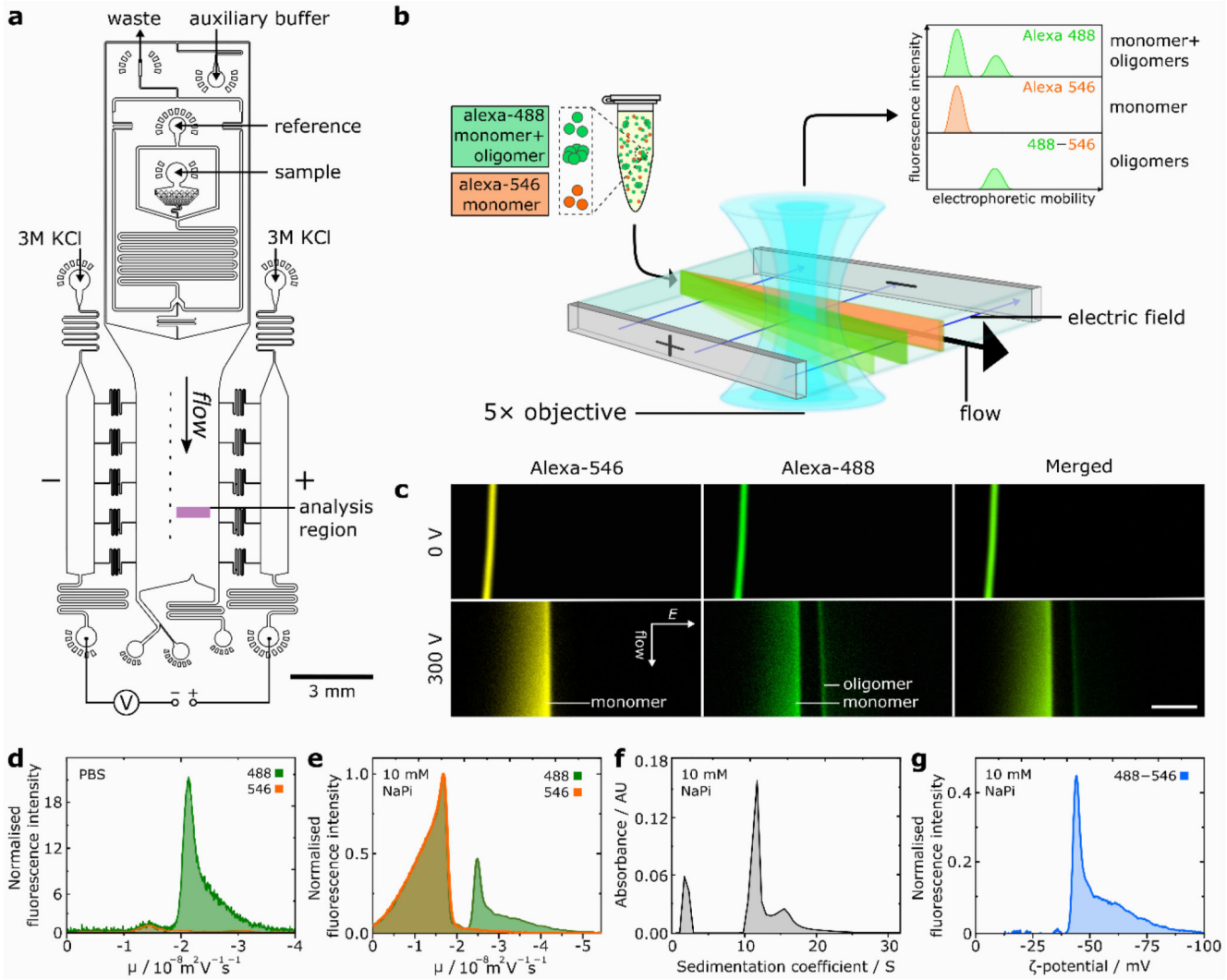

Figure 1.

(a) Schematic of device design for desalting-μFFE. The device operates through liquid KCl electrodes, allowing voltage application downstream of the electrophoresis chamber to prevent disruption of flow by electrolysis products.[18] Reference sample can be introduced on-chip in pure water diluent, enabling rapid in-situ sample desalting prior to downstream electrophoresis. (b) Schematic for two-colour microfluidic free-flow electrophoresis of oligomeric αS. (c) Fluorescence images of Alexa546-labelled αS monomer reference and Alexa488-labelled oligomeric mixture undergoing μFFE in 10 mM sodium phosphate (NaPi) buffer (pH 7.4). Direction of fluid flow and electric field (*E*) shown by arrows, scale bar = 300 μm. (d) Electropherograms for Alexa546 monomer reference and Alexa488-labelled αS oligomeric mixture fluorescence in PBS buffer. (e) Electropherograms for αS monomer and oligomeric mixture in 10 mM NaPi buffer. (f) AUC data for the same oligomer sample for data shown in (e), the peak at S ≈ 2 is due to monomeric protein. (g) Distribution of oligomer ζ-potential.

Europe PMC Funders Author Manuscripts

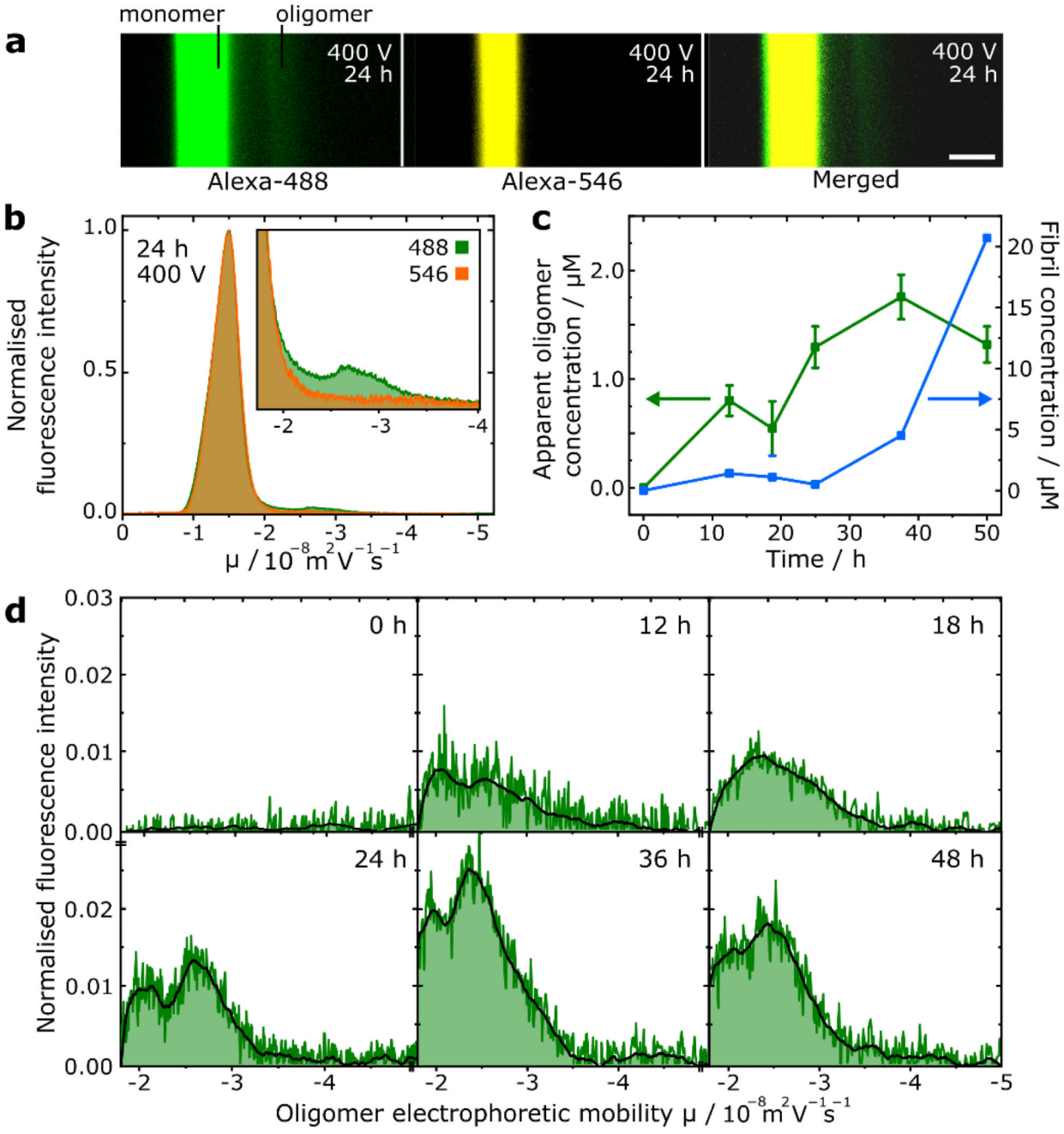

Figure 2.

(a) Fluorescence images of μFFE experiment of transient oligomers formed after 24 h αS aggregation. Scale bar = 300 μm. (b) Superimposed electropherograms of normalised alexa-488 and 546 fluorescence for micrographs shown in (a), (inset) magnification of electropherograms showing oligomeric region. (c) Scatter plot showing progression of oligomer concentration (monomer equivalents) and extent of monomer to fibril conversion (fibril concentration in monomer equivalents) over the sampled time points. Error bars correspond to standard deviation of three repeat measurements of the same sample. (d)

Electropherograms and smoothed traces corresponding to oligomeric species only at each sampled aggregation time point.

Europe PMC Funders Author Manuscripts

Europe PMC Funders Author Manuscripts

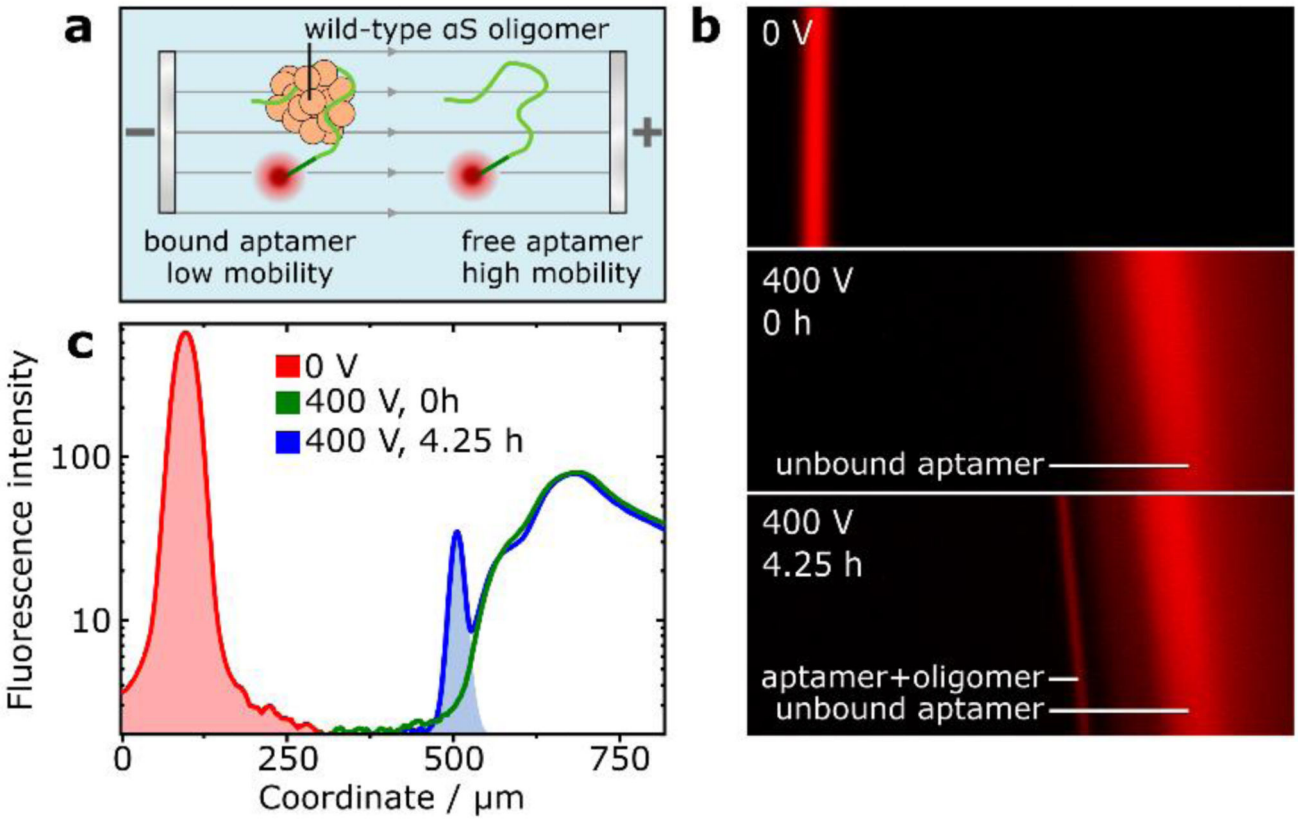

Figure 3.

(a) Schematic for fractionation of oligomer-bound and unbound aptamer by μFFE. (b) Images of aptamer fluorescence during μFFE, from aptamer mixed into an aggregation reaction of wild-type αS at 0 h and 4.25 h timepoints. Additional, lower-mobility fraction after 4.25 h indicates aptamer-oligomer binding. (c) Analysis and integration of aptamer electropherograms enable approximation of the concentration of aptamer-bound oligomers.